DOCTOR OF PHILOSOPHY

Identification of measurable metrics for characterisation of marine turbulent coherent structures in tidal races

Lucas, Natasha

Award date:
2021

Awarding institution:
Bangor University

Identification of measurable metrics for characterisation of marine turbulent coherent structures in tidal races

N. S. Lucas

PRIFYSGOL
BANGOR
UNIVERSITY

School of Ocean Sciences
College of Environmental Sciences and Engineering

Submitted in partial satisfaction of the requirements for the
Degree of Doctor of Philosophy in Physical Oceanography.

Supervisor Dr. M. Austin

June, 2021

Abstract

High Reynolds number tidal race environments, attractive for development of in-stream tidal energy generation, are known to contain Coherent Structures. Coherent structures are turbulent boundary layer structures that translate vertically through the water column and are expressed on the surface as boils. Their local vorticity over small distances and large velocity shear contribute to high mechanical failure rates of tidal energy turbines. These coherent structures are also known to transport sediments, pollution, and phytoplankton blooms. Metrics for measuring these phenomena are not well defined. Many studies of marine potential energy sites have used the standard International Electrotechnical Commission (IEC) metric for quantifying turbulence at wind sites; the turbulence intensity. However, discrepancies in turbulence intensity and power densities in marine environments suggest that this metric does not capture coherent structure information as such, new metrics appropriate to water turbine design and prediction of fatigue loads are needed. The aim of this thesis is to develop and test new methodologies, using measurements from an off-the-shelf ADCP correlated with visual quantification of surface boils, to provide a more appropriate and comprehensive characterisation of turbulence at the scales, structure/coherency and stress which are most likely to compromise the structural integrity of the tidal energy infrastructure and its operational performance.

Acknowledgements

I'd like to thank my dogs.. for their unwavering tail wagging throughout dull days of writing! Also to Ben Powell, without your skills there would be no MTO. Lastly to Tom Rippeth, for having faith in me from the outset and always supporting me.

This project was supported by Knowledge Economy Skills Scholarship (KESS2, 80815 / BUK2108) led by Bangor University on behalf of the Welsh higher education sector through funding from the Welsh European Funding Office (WEFO), the European Social Fund (ESF) and the company partner Nortek-AS, Norway. https://www.nortekgroup.com/

Contents

List of Figures

Abbreviations & Nomenclature

α	anisotropy ratio
δ	boundary layer thickness
ε	turbulence kinetic energy dissipation (the local rate of destruction of turbulent energy by viscous forces)
η	Kolmogorov microscale, $(\eta = (\nu^3/\varepsilon)^{1/4})$
Γ	body force or external source
γ	intermittency factor, ratio of CS burst duration to burst period
κ	von Kármán constant, $\kappa = 0.41$
$\mathbb{R}$	Reynolds Stress tensor
μ	viscosity
ν	kinematic viscosity, $\nu = \frac{\mu}{\rho_0}$
$\overline{\gamma^2}$	mean squared strain rate
$\overline{u}$	mean velocity
$\overline{W}$	vertical mean flow
Φ	TKE = $q^2/2$
ρ	density
τ	turbulent shear stress
A	anisotropy magnitude
c_p	specific heat capacity
F	rate of CS bursts per unit width and time
g	gravitational acceleration

H	water depth
II	a principal invariant of the anisotropy tensor
K	non-dimensional pressure gradient
k	wavenumber
L	length scale
Q	kinematic heat flux
T'	fluctuating temperature
T_0	surface temperature
U	flow velocity
u', v', w'	fluctuating velocity components along the longitudinal (x), lateral (y) and vertical (z) directions, where $< u' >= 0$ and so forth
u_*	friction or shearing velocity
U_i	average velocity component
z	depth from the boundary/ height above ground scale
z_0	roughness length scale which depends on the size of the boundary roughness
ABL	Atmospheric Boundary Layer
ADV	Acoustic Doppler Velocimeter
AUV	Autonomous Underwater Vehicle
BBL	Bottom Boundary Layer
cf.	short for the Latin: confer/conferatur; "to compare with"
CS	Coherent Structures
CTKE	Coherent Turbulent Kinetic Energy
FLY	Fast Light Yo-yo
HWA	Hot Wire Anemometers

IR	Infrared
MTO	Menai Turbulence Observatory
N-S	Navier-Stokes equations
OBL	Oceanic Boundary Layer
PDF	Probability Distribution Function
SF	Structure Function = D(z,r)
TEC	Tidal Energy Converters
TKE	Turbulent Kinetic Energy
w.r.t.	with respect to

Chapter 1

Introduction & Literature Review

1.1 Introduction

The United Nations Framework Convention on Climate Change (Secretariat, 1994) convened in March 1994 and currently has 197 countries ratifying the convention. It binds member states to act to prevent dangerous human interference with the climate system by stabilising greenhouse gas concentrations “at a level that would prevent dangerous anthropogenic (human induced) interference with the climate system." Stating that "such a level should be achieved within a time-frame sufficient to allow ecosystems to adapt naturally to climate change, to ensure that food production is not threatened, and to enable economic development to proceed in a sustainable manner."

Two operational outputs from this convention were the Kyoto protocol and the Paris Agreement. The former asked countries to adopt policies and measures for mitigation. It entered into force in 2005 with commitments until 2020 following the Doha Amendment. It suggested decarbonising the global power sector by 60-70% from current levels (Secretariat, 1998). The latter and more well-known Paris Agreement was a legally binding international treaty on climate change adopted in November 2016 by 196 parties to limit global warming to 1.5 degrees Celsius compared to pre-industrial levels. This agreement works on a 5 year cycle, fed with knowledge from the Intergovernmental Panel on Climate Change (IPCC); the United Nations body for assessing the science related to climate change.

This convention is a powerful driver for the provision of renewable energy. One such resource is that of principally unexploited marine tidal energy. In the UK it is estimated that annual usage of electricity is 300 TWeh/year, applying Bets Law and pragmatic device deployment it is estimated that approximately 5% of that could be fulfilled with tidal stream devices,

(Hardisty, 2008), thus the shallow shelf seas hugging the UK coastline have seen an emergence of industrial interest in diagnosing and developing a new tidal energy industry.

Tidal races (tidal environments that could potentially produce a high yield for Tidal Energy Converter (TEC) devices) are challenging environments, with strong currents and turbulent flows. Design of infrastructure robust enough to survive in these highly turbulent environments remains a major challenge to the development of this industry and as such optimisation of devices to be deployed in these flows is a requirement for sufficient yields to be attained.

Within these turbulent flows coherent structures (CS) are often observed; known as boils as their turbulent signature impinges on the surface. Similar problems were encountered in the development of the more advanced wind energy sector where, turbulence and in particular larger scale coherent structures are found to be a major contributor to large load excursions on turbine blades as they contain large velocity shears and significant local vorticity over small distances, inducing a broadband aeroelastic response in the turbine rotor increasing fatigue damage, (Kelley et al., 2000).

This work aims to develop new methodologies for the measurement of large turbulence parameters associated with coherent structures in the marine environment, implementing an experimental regime by way of an observatory in the Menai Straits (Anglesey, UK), hereafter the Menai Turbulence Observatory (MTO). This will be achieved by utilising correlation of measurements from high resolution surface cameras and acoustic marine measurements, allowing characterisation and quantification of CS and then continues with definition of the turbulence metrics needed to determine flow structure, thus supporting the optimisation of devices and deployment locations.

This thesis is presented in paper format, commencing with a brief review of current and proposed TEC devices, moving on to how turbulence is measured in the marine environment (with a summary of the most pertinent foundations of turbulence theory in the Appendix, if required). It then follows with an investigation of one of the constraints of tidal stream devices; that of coherent structures (CS) impinging on the devices and inducing fatigue related wear and tear. This section first identifies these structures from theoretical and laboratory standpoints, moving on to subsections emphasising identification of these structures in environmental flows and their effects on TEC devices. Once these background topics have been covered,

the methodology used in the papers is addressed and subsequently two papers are presented that contribute to the field. The work then concludes with a discussion and implications for further research.

1.2 Tidal Energy Converters

This thesis does not directly deal with TEC devices, but as the thrust of the work is to understand flow structures that impact on TEC devices, this thesis starts with an overview of what they are and how they work.

There are many types of ocean tidal energy devices proposed, the most prevalent being horizontal and vertical axis turbines, oscillating hydrofoils, Archimedes screws and tidal kites; a good illustration of the schematics of such devices can be found here: http://www.emec.org.uk/marine-energy/tidal-devices. However, with a loading density of water being $\sim$800 times that of air one is not able to simply 'steal' technological intellect from the wind energy sector. In fact, of the devices that have been tested in the field not all have been successful, for example a turbine deployed in the Bay of Fundy by OpenHydro with an 18 month plan had to be extracted after 6 due to unexpected turbulent conditions. This highlights the need for testing and site characterisation prior to instalment especially as tidal turbines, despite blades being smaller for the same energy yield, are more expensive than their wind counterparts. Tidal currents increase with distance from the bottom and kinetic power density scales with v^3, so the siting of tidal power turbines is another important consideration. Moreover, these tidal turbines are deployed in more adverse environments so maintenance and repair can be extremely difficult and hazardous.

The TKE signature of coherent structures in particular is thought to adversely affect mechanical loads leading to gear box failures (McCaffrey, 2018) with Kelley et al. (2005) finding 1:1 correlation between the vibrational response of turbine blades and the coherent TKE spectral frequencies, coined 'resonant coupling' and thought to be the reason for fatigue damage of the blades in wind turbines.

Many reviews have been written on the current state of the market with respect to TEC devices. It is disadvantageous to reiterate these works, so instead the reader is directed to the following: Uihlein et al. (2016) provides a review on the current state of research in ocean energy, with sections covering; resource assessment, environmental impacts, socio-economic impacts, grid

integration, installation and legal affairs. Milne et al. (2016) provides an extremely detailed review of hydrodynamic loads on tidal turbines due to turbulence, with many of the references therein pertinent to CS; covered in detail later in this work. They look at observations and metrics, (particularly with reference to scales encountered at hub height), sensors, models and also loading and amplification of flow over rotor blades in great detail. Day et al. (2015) provides a thorough review on the issues that scientists may encounter when modelling marine renewable energy systems, including wind, wave and tidal.

As this is a rapidly growing and changing field it is not beneficial to detail individual capabilities, in fact in the writing of this work the market has already changed, so instead the reader is directed to these web resources for those wishing to review the current projects, technologies and TEC companies, both for the UK and globally:

http://en.openei.org/wiki/Marine_and_Hydrokinetic_Technology_Database
This site has an interactive map of current resources globally for wave, tidal, current and ocean thermal energy, broken down into current technological phase such as proposed, in development, testing and deployed.

https://www.renewableuk.com/page/UKMED2
This links to an interactive database of wave and tidal energy projects within the UK, also delineated by technological phase.

and lastly http://www.energybc.ca/tidal.html
links to an extremely thorough, recent and well researched site on tidal energy (with links to all other energy profiles) from Canadian counterparts, including a very informative image illustrating the estimate of global tidal resource, depth and potential power output, across the globe.

1.3 Measuring Turbulence Within the Marine Environment

Advances in technology in recent years have allowed the direct measurement of dissipation of turbulent kinetic energy. These measurements have largely been based on free-falling microstructure profilers, however these measurements are labour intensive and costly requiring a dedicated ship. Further advancements by way of ocean microstructure gliders has improved the free-falling probes sparse and intermittent measurements, rarely exceeding 1-2 days, but

they are still limited to deployments in the order of weeks or months. These limitations led to developments of new techniques based on standard off-the-shelf ADCPs which can be moored to provide much longer time series of turbulence parameters.

Acoustic Doppler current profilers (ADCP) are instruments that utilise acoustic sonar pulses from scatterers in the water column to measure mean currents, shear and turbulent flow in the marine environment. Broadband technology, now widely employed in high frequency ADCPs, utilises phase shift in acoustic signal rather than the Doppler frequency shift of older Narrowband technology, allowing a greater accuracy in estimation of the 'scatterer' contraction or dilation.

ADCPs range from single to multiple transducers, with vertical or oblique angled 'Janus' beams. When beams number more than three, components of the velocities are able to be elucidated giving Earth coordinates; east, north and up, of the flow field at varying distances from the ADCP transducer head, known hereafter as 'bins'.

Moreover, if the flow field is measured in beam coordinates rather than being converted to Earth coordinates on-board, additional parameters can be obtained such as ε along beam from Structure Functions (Lucas et al., 2014; Wiles et al., 2006) and Reynolds stresses and TKE production within the beam volumes from the variance method Lohrmann et al. (1990), Lu et al. (1999), Rippeth et al. (2002) and Stacey et al. (1999). Further, if a vertical beam is available concurrently with Janus beams, as is now possible with recent advancements in ADCP technology, one can obtain previously unavailable components of $\mathbb{R}$ in oceanographic flows due to the exact solutions of vertical velocities Dewey et al. (2007).

The variance method and relies on the fact that the flow is homogeneous over the beam spread and that the values of the tilt angle of the instrument to the horizontal are small, with tilt angles $< 8^\circ$ leaving approximations being correct within 99%, (Lohrmann et al., 1990). However this assumption has since been challenged in the presence of waves, (Rippeth et al., 2003), with the statement that tilt angles of 2.5° can lead to a bias of these stresses by 20-30%, (this is also mentioned in earlier works by Heathershaw (1979)). In fact Lohrmann et al. (1990) do explore no-tilt assumptions in detail in their appendix, where they comment that correlation term in the horizontal, $\overline{u'v'}$, is usually small compared to the Reynolds stresses. If it were of the same order of magnitude with no tilt then the contamination of estimates the stress

components would be small (using this methodology) but that these assumptions are incorrect if surface gravity waves and/or internal waves are present (Lohrmann et al., 1990; Rippeth et al., 2003; Scannell et al., 2017).

These techniques essentially measure the 'dissipation scales' of turbulence i.e. the small-scale end of the turbulent cascade, sometimes smoothing out the large-scale variability. They do not capture the detail of the coherent structures inherent in the pathway of TKE from generation scales to dissipation's associated with the transfer of momentum from the mean flow to turbulence, details of which are needed for field assessments of the potential impact on TEC infrastructure.

1.4 A review of Coherent Structures

> " The occurrence of CS in the proposed MTO observations are linked to the formation of vortices downstream of rough seabed topography leading to the ejection of turbulence from the turbulent boundary layer close to the sea bed. The surface manifestation of sub-surface coherent structures, "boils", are commonly observed in regions of strong flow such as rivers and strong tidal flows." (KESS2 project definition)

Fluid motions near boundaries were first coined as boundary-layer hypotheses back in 1904 by Prandtl (1904), where he suggested that viscosity effects fluid motions and 'wall regions' which were coined as a combination of a viscous sublayer and a buffer region. This wall region characterises generation, maintenance and transport of turbulence phenomena. Strong anisotropy is found in the turbulence in boundary layers and ejection of fluid elements from this wall region are common and have been characterised as 'coherent structures'; these are three-dimensional disturbances which have a well defined character independent of mean flow parameters, however their intensity and frequency of occurrence are a measurable function of these parameters.

Many texts since have considered coherent structures and the mechanism of their formation. In many of these texts it has been the theoretical approach of fluid dynamics that has been studied, rather than the physical aspects which characterise these flows, as obtaining both the spatial and synoptic information needed for measurement of these phenomena has proven difficult.

An early work making visual studies of the wall region within pipe flow in laboratory experiments was by Corino et al. (1969). Their seminal work reviewed previous theories by

Bakewell (1966), Black (1968), Einstein et al. (1955), Ferrari (1959), Grant (1957), Kline et al. (1967), Landahl (1967), Malkus (1956), Phillips (1967), Schubert et al. (1967), Sternberg (1967), Townsend (1956, 1958, 1961), Willmarth et al. (1967) and Wills (1967) and compared and contrasted results to characterise these ejections. Their study observed large elongated streamwise eddy structures forming and bringing with them an updraft of the fluid between this structure and the boundary.

This occurrence is common, the formation of which is explained by various methods; pressure gradients and fluctuations (Ferrari, 1959; Grant, 1957), two-layer velocities (Mitchell et al., 1966; Willmarth et al., 1967, 1962), instabilities from vortex stretching (Black, 1968; Ferrari, 1959), fluid jets from turbulent wakes (Grant, 1957). Indeed Grant (1957) hypothesized that energy from the mean flow to turbulent energy favors components aligned with the direction of vortex stretching. This preferential stretching brings about a stress in the wake of the vortex which must be relieved; thus so by ejection of fluid elements. Corino et al. (1969) study observed that there was periodic ejection of fluid elements from the region adjacent to the sublayer, with an zone of high shear at the interface between the main flow and decelerated eddy region giving rise to ejected elements. These observations fit with theory (Bradshaw, 1967) that coherent ejections do not predominantly originate from the viscous sublayer, but rather from the region outside of this and are thus not dependent on wall conditions, this is further discussed in detail in the work of Kistler (1962). Corino et al. (1969) work shows that the innermost sublayer is essentially passive and the rest active, with interactions between regions occurring in both directions. This theory is further developed later in the context of wall similarity in the review by Raupach et al. (1991)

Corino et al. (1969) work culminated in a broad agreement with the views of Bakewell (1966), Ferrari (1959), Grant (1957), Mitchell et al. (1966), Townsend (1958) and Willmarth et al. (1967, 1962) of a picture of coherent structure formation; shear layer formation bringing about a two-layer velocity which leads to an ejection. Eddy size increases with distance from the generation region up to a scale distance whereby eddy growth and relative motions proceed at a diminished rate. Thus eddies are often not indicative of a wall region at a particular time or axial position, but rather dependent on what occurred upstream and could be illustrative of how mean flow affects location conditions producing coherent ejections.

At a similar time Kovasznay (1970) reviewed the experimental analysis of these same bursting phenomena, with particular attention paid to the works of Favre et al. (1967) and Tritton (1966). Kovasznay (1970) looks more at the experimental analysis of these phenomena rather than the detailed turbulence theory behind them. He focuses on the use of Hot Wire Anemometers (HWA), which were the leading measurement option of the era, concentrating on velocity correlations to ascertain anisotropy. Of note is the ability of HWA's to obtain space correlations in three velocity components, as studied by Tritton (1966) without temporal behaviour being ascertained. Kline et al. (1967) used the novel technique of water analysis, using a hydrogen bubble technique and then combining this with HWA for space-time information, as described in Kim et al. (1971). Corino et al. (1969) is also mentioned for obtaining the same results with different techniques and also for obtaining lateral spacing of the structures, Kovasznay (1970) summarised that:

> "The general picture of the turbulent motion one can put together from this mass of experimental information is still not decisive but highly suggestive. Both close to the wall inside or near the sublayer and also at the free stream there appears a random sequence of "eruptions" or "bursts." The smallest ones occur in the outer part of the viscous sublayer and their trajectory can be followed to some distance into the fully turbulent wall layer, where they seem to lose their identity. At the outer intermittent region, similar but larger bursts were observed and they appear to be highly correlated with the large-scale motion of the fully turbulent interior so they can be regarded as the "footprints" of the interior eddies."

Kovasznay (1970) concludes with space-time correlation maps (both auto and cross correlation), and explores the dependence of intermittency with the mean pressure gradient, (as also explored by Fiedler et al. (1966)), where the intermittency increases with negative streamwise pressure gradient and decreases otherwise, thus seemingly controlling the burst rate near the wall regions. He confirms Corino et al. (1969) supposition in that bursts appear in distinct streaks whose lateral spacing, z_0 is approximately:

$$\frac{z_0 u_*}{\nu} = 100 \tag{1.1}$$

With the rate of bursts per unit width and unit time:

$$F = F_0 \, \frac{u_*^3}{\nu^2} \, (K - K_0)^2 \tag{1.2}$$

i.e. the number of large bursts per unit width and time reaching the outer region of the layer is proportional to F, which depends on the friction velocity and pressure gradient.

1.4.1 Coherent Structures within Environmental Flows

Some of the first measurements of coherent structures (CS) within environmental flows were carried out in atmospheric boundary layers (ABL), one of the most notable was by Kaimal et al. (1972) where he analysed, as part of the Kansas (Izumi, 1971) experiments over a smooth wall, spectra and cospectra of turbulence in the framework of similarity theory and compared these results with other atmospheric and oceanographic investigations. Instrumentation included HWA, sonic anemometers, thermometers, and drag plates to obtain surface stresses. Full experimental details can be found in Haugen et al. (1971).

Kaimal et al. (1972) utilised the approach of collapsing all spectra into universal curves in the inertial subrange and then observed the spectral behaviors, finding consistent spectral fall within these inertial subranges for both spectra and cospectra. They found that the curves spread out according to z/L at the lower frequency end of the spectrum, where the anisotropy of the turbulence is manifested.

The use of similarity theory however can have misgivings above the range $|z/L| \leq 1-2$ when the measurement height is much less than the depth of the flow or thickness of the boundary layer, or over inhomogeneous surfaces (Foken, 2008; Walter et al., 2011).

Raupach et al. (1991) give an excellent review of boundary layer exchange processes and the prevalence of coherent structures when analysing atmospheric boundary layers over rough walls. They spend much of their text studying the interaction between the inner and outer regions of a turbulent boundary layer, including within the roughness element of canopies. They define each area as; the outer inertial or logarithmic region with a lengthscale of boundary layer thickness, δ, and an inner roughness/viscous sublayer region where the lengthscale is $\nu/u*$. In our current context the extra 'within canopies' detail need not be included, as we are looking at bare seabeds, but future studies may indeed have analogies of grasses and tree canopies to that of seaweeds and sea-grasses.

So, above the roughness sublayer, Raupach et al. (1991) explore three hypotheses in detail (wall-similarity, equilibrium-layer, and attached-eddy hypotheses) for length and velocity scales, leading to predictions for turbulence length scales and velocity variances.

They find, through rigorous analysis of many studies, that "wall similarity" holds, which is defined as:

> Outside the roughness (or viscous) sublayer, the turbulent motions in a boundary layer at high Reynolds number are independent of the wall roughness and the viscosity, except for the role of the wall in setting the velocity scale u^*, the height Z = z — d and the boundary-layer thickness δ.

Wall similarity hypothesis is indeed supported by experimental evidence with stress to shear relationships, single-point velocity moments and two-point velocity covariances, explained within the text.

Of particular interest to our current study is their scrutiny of turbulent organised motion (coherent structures). Firstly Raupach et al. (1991) review literature on smooth-wall boundaries and then explore rough-wall boundary layers. They utilise two-point velocity correlation functions to yield eddy length scales, orientation and convection velocities, finding that vertical inhomogeneity and horizontal homogeneity has a maximum correlation along the x-z plane sloping at $\sim 18deg$ which are inclined structures leaning with the shear with a z-correlation at zero time delay, thus concluding that organised fluctuations are aligned vertically. However, they inform the reader that these are only weak indicators of coherent structure flow fields. They then follow with a review focus on four types of structure in organised motion: (a) low-speed streaks; (b) ejections and sweeps; (c) ramp-jump structures in velocity and temperature signals; and (d) large-scale, outer-layer motions.

They find that the former, (a), is mainly a smooth-wall phenomena. Ejections and sweeps, (b), however are identified in the 'bursting process' of CS over rough-walls, albeit believed to be sourced by different phenomena for smooth and rough walls; the former being an ejection sequence that draws on the viscous sublayer and the latter that of the low-momentum fluid trapped between roughness elements. These ejections over rough-walls are thought to be the CS that are identifiable thorough much of the flow, (Grass, 1971). Nakagawa et al. (1977) find that these intermittent events have a sweep to ejection ratio that increases close to the boundary

and with increasing roughness, and both these authors, Raupach et al. (1991), and others therein, find that there is a link between organised motion defined in this way and the TKE budget that can be obtained using cumulant discard analysis, relating the normalised third velocity moments (or skewnesses) to the difference between sweep and ejection contributions to stress.

Ramp-jump, (c), structures, also commonly known as sawtooth patterns have been universally observed by many authors throughout smooth and rough wall boundary layers in both temperature and velocity fields, which are found to be predominantly the signature of organised large-scale shear driven motion. Indeed the shape of two-point correlation functions in velocity and temperature are found to be substantially determined by these structures.

Importantly, there is found to be an association between ramp-jumps and sweeps dominating momentum transfer. Gao et al. (1989) ensemble average potential temperature and velocity fields in slightly unstable conditions and find a microfront in temperature and vertical velocity with the shift in sign of the vertical velocity occurring almost simultaneously at all levels, while the thermal front lower levels lag behind the upper. This is attributed to the temperature fluctuations being associated with a physical transport of air while velocity fluctuations propagate rapidly, being dynamically related to pressure perturbations. These microfronts are observed with sweep motions just behind and ejection just ahead of this front, consistent with quadrant-analysis results. These events in this study account for over 75% of the heat and momentum transfer while only occupying 33% of the time (although the ensemble averaging and 2D slices mean these results must be treated with caution). However, Robinson (1990) found similar 3D structures in numerically simulated smooth wall boundary layers alongside Λ-vortices.

And so onto large-scale outer-layer motions, (d). Wall similarity states that CS should be self similar in outer and inner rough and smooth wall boundary layers. This is supported Antonia et al. (1972), Corrsin et al. (1955) and Kovasznay (1970). In summary, Raupach et al. (1991) postulate that flow at the boundary is dominated by an intense shear layer with an inviscid (Rayleigh) instability associated, leading to rapidly growing transverse vorticity perturbations (with typical streamwise wavelengths proportional to local layer depth, $\sim 8h$). These motions and subsequent 3D secondary instabilities are the likely progenitors of the fully developed

turbulence field from the boundary. This field retains it's length scale signature leading to Λ-vortex structures. (Baylyl et al., 1988; Pierrehumbert et al., 1982; Raupach et al., 1991; Wygnanski et al., 1970)

So we now move from discussions in an ABL to an Oceanic Boundary Layer (OBL). Heathershaw (1974) inspected the sweep and ejection signs and magnitudes of u and w w.r.t. the bursting process of intermittent CS with further analysis finding that ejections are preceded with a deceleration of the horizontal flow, and a sweep after an acceleration. Analysing the departure of these distributions from Gaussian behavior he found that the negative skewness characterised the asymmetry of uw and a net positive input of Reynolds stress, and with further scrutiny it is possible to determine contributions of ejection and sweep events to the Reynolds stress via the outliers within -2 or -3 standard deviations, supporting the view put forward by Corino et al. (1969) that as much as 70% of the Reynolds stress may be derived from ejection events alone (dependent on the Reynolds Number). He finishes with durations of events, finding that ejections are about 1/3 more intense than sweeps and exist for 20% less time, with durations being $\sim 5-10s$ in length separated by $\sim 20-100s$, corresponding with observed maxima in the Reynolds stress cospectrum as observed by Bowden et al. (1956).

Heathershaw (1979) did a follow up study to this analysing Reynolds stress cospectra and normalised wavenumber spectra of the horizontal and vertical velocity fluctuations, focusing on the kurtosis and skewness factors, differences between ABL and OBL and the effect of suspended sediments. Within the areas studied of interest to this current text and not already described above, Heathershaw (1979) finds that although the boundary layers of ABL and OBL are similar in terms of scaled spectra and Reynolds stress, this structural similarity (motion that contributes to the Reynolds stress, defined as similarity scaling above) is not as defined when looking at the stress tensor components, and that this is more evident in deep flows. Heathershaw (1979) finishes with the supposition that these flows may be structurally similar in shallow flows such as the Menai Strait, which is supported by the findings of Gordon et al. (1973) who worked in a narrow tidal channel and found a linear relationship between the Reynolds stress, $\mathbb{R}$, and the TKE $1/2\rho\overline{q^2}$. This suggests that for tidal channel energy sites the ABL and laboratory scalings may still hold, but this should be taken with caution when studying sites with greater depths.

Heathershaw (1979) obtains evidence to support the work of Bowden (1962) and Soulsby (1977) that the bulk of the energy in the vertical motions is contained at wavenumbers in the range $10^{-1} < k^* < 10^2$, with $k^* = kz$ the non-dimensional wavenumber, and k being the radian wave number, and that the bulk of the Reynolds stress is contributed by motions in the wavenumber range $10^{-2} < k^* < 10^1$. He also finds increasing isotropy with increasing distance from the boundary and obtains an intermittency factor, γ (ratio of burst duration to burst period), of $0.25 < \gamma < 0.33$, which is similar to other reviewed work therein.

Noteworthy, Heathershaw (1979) finds a discrepancy between turbulent energy dissipation and production, the former exceeding that later by a factor of $\sim$5 at z = 1m, and that using standard definitions (pages 405-406) he is able to derive a typical dissipation wavenumber, which he finds to be $\sim \mathcal{O}(3)$ larger than the highest wavenumber observed in the u, w and uw spectra. Heathershaw (1979) notes the interest in further studying the role of the energy budget in the boundary layer.

Further evidence of the limits to the applicability of ABL similarity scaling particularly w.r.t. spectral energy densities and momentum fluxes is made much later by Walter et al. (2011). Walter et al. (2011) find that spectra were more energetic than the Kaimal et al. (1972) curves at the low frequency end of the spectrum, which is attributed to rough upstream conditions, spectral lag and large eddy readjustment. Long meandering 'superstructures' are mentioned to be possible contributions. These differences in energetics results in momentum flux cospectra underestimating stresses in this frequency range. Consideration of length scales in this study also suggests that depth could be a limiting factor, that Kaimal et al. (1972) curves may only apply when the measurement height is much less than the depth of flow or boundary layer thickness. Interestingly though, Walter et al. (2011) also finds a mismatch of production to dissipation of TKE, which warrants further investigation.

Lastly, and of particular interest to further studies, Heathershaw (1979) reflects on the asymmetry in the ratio $\mathbb{R}/\overline{q^2}$ over a tidal cycle, with reference to Johns (1969) work, showing that phase differences between the turbulent shear stresses and the mean velocity gradients may modify the horizontal current structure and energy dissipation. This is relevant for tidal energy generation in open sea sites, being productive at certain phases of the tide and at deeper sites than our Menai Turbulence Observatory. Heathershaw (1979) quotes (Townsend, 1976,

p. 123) in his supposition of 'inactive' motions from adverse pressure gradients contributing to $\overline{q^2}$ but not to $\mathbb{R}$.

Building on the theoretical considerations, efforts have been made to characterise coherent structures in the environment. Nimmo Smith et al. (1999) published a study looking at turbulent boils in the well mixed open ocean of the North Sea with an interest in how this turbulence contributes to replacement of surface waters from depth enhancing vertical fluxes, sediment concentration and how these boils influence the spreading of surface pollution such as oil spills. They use an upward pointing side-scan sonar and obtain video image frames and spectrographic images from an overflying aircraft.

Their study quantifies the boil speeds (w.r.t mean flow) and sizes for the region, generalising the latter using the water depth. They find that from a flat sea bed boils are incident on the surface with a diameter of 0.9 ± 0.2 times the water depth, with each boil lasting for at least 7 minutes and traveling with velocities different from that of the combined tidal and wind-drift surface currents (boil velocities of $0.89 \pm 0.09\ ms^{-1}$ c.f. currents at 17m depth of $0.98 \pm 0.03\ ms^{-1}$). They quote Heathershaw (1974) in the ejections from the bottom boundary layer (BBL) reaching vertical speeds of 25% of the forcing current, and find that the surface expression is tidally dependent.

They find that these surface eddy sizes do vary consistently with laboratory measurements in that the separation and size are shown to depend on U, H, u^* and ν, consistent with Corino et al. (1969). The limitations of side scan sonar to measure these boils on the surface are limited by bubbles being produced at the upwind boundary.

Nimmo Smith et al. (1999) touch on the morphology of these boils on the surface being counter-rotating eddies, which is then expanded on by Thorpe et al. (2008) with measurements in the eastern Irish Sea using a side-scan sonar with concurrent dissipation measurements vertically using a Fast Light Yo-yo (FLY) profiler and horizontally using an Autonomous Underwater Vehicle (AUV). This surface morphology, as previously seen by (Kumar et al., 1998; Nimmo Smith, 2000), with eddy centers being roughly aligned across the flow and with dimensions greater across the tidal flow than along it, is hypothesised to be eddy pairs of two legs of the Λ-vortices meeting at the sea surface.

Using this setup Nimmo Smith et al. (1999) are able to relate the boil incidence with turbulence levels and find that boils are continually present when ε exceeds $3x10^{-6}\ WKg^{-1}$ compared with background levels of $1x10^{-7}\ WKg^{-1}$ and that boils incident on the surface are shortly followed by increased turbulence, with horizontal dimensions of $\sim 25m$ and $\sim 5-9m$ for boils and turbulence respectively. They also find a displacement of the AUV corresponding to vertical motions which are concurrent with fall speeds of the FLY which is consistent with the presence of large, energetic eddies with vertical velocities during periods of high dissipation, although they are not able to quantify vertical velocities from these. They also discuss stratification and horizontal tidal straining effects which are not relevant for this current review.

Their study estimates boil dimensions along-tide of $(0.51 \pm 0.225)H$, and the across-tide dimension is $(0.58 \pm 0.29)H$, where H is the water depth, which is less than that of the previous study, with a peak in PDFs of along to across tide ratios of boil widths measured of 0.75, consistent with the eddy pair hypothesis, although the mean is 1. They interpret the large-eddy structure as intermittent coherent features of $\sim 7m$ scale moving upwards through the water column carrying small-scale turbulent motions from the bed to the surface where they then diverge horizontally to form boil features with dimensions half that of the water depth.

Again, the side-scan sonar has limitations in measurement at the surface, as per the last study but also in this scenario in measurement of boil dimensions at the surface. To try and overcome these limitations, Chickadel et al. (2009, 2011) and Talke et al. (2013) have done a series of experiments at different riverine locations using surface infrared (IR) imaging under the 'Coherent Structures in Rivers and Estuaries Experimental Regime', (COHSTREX).

Chickadel et al. (2009) first quantify boil locations and diameters vertically propagated from a fixed sill and compare these with a model developed based on vertical propagation of a vortex dipole, hypothesising that boils self-propagate to the surface via a vortex-pair interaction, modelled as a 2D vortex-dipole. Chickadel et al. (2011) and Talke et al. (2013) follows this with flow and turbulence at the water surface based on disruption of the cool skin layer and finish with an extremely detailed analysis of CS and boils from dune-like riverbed to surface manifestations.

The methods employed are not directly relevant to TEC studies as Chickadel et al. (2009, 2011) and Talke et al. (2013) investigations are carried out in predominantly quiescent stratified environments, transporting water masses of different density signatures to a calm surface cool skin with little wave contamination; their analysis of the boil morphology at the surface is unprecedented. However, many of Chickadel et al. (2009, 2011) and Talke et al. (2013) findings are directly relevant to this study. Chickadel et al. (2009, 2011) and Talke et al. (2013) add weight to the kinematic model of Λ-vortex loops and shed light on the surface expressions of boils vorticity; with the vigorous upwelling, surface deflection and spreading having little vertical velocity variance, but with secondary eddies with vertical vorticity at the perimeters. They find that upwelling at the center of the boils, (negative dw/dz), restricted by the kinematic surface boundary condition, is associated with convergence (positive dw/dz) and downwelling at the periphery (and ambient flow) and a considerable redistribution of TKE.

Chickadel et al. (2009, 2011) and Talke et al. (2013) confirm the hypotheses of Thorpe et al. (2008) in that large scale eddies of low momentum and higher variance, (finding an average boil velocity of 4% slower than the ambient flow), transport smaller vortices upward, and they quantitatively link the TKE redistribution from BBL, (where production exceeds dissipation, found in Talke et al. (2013)) to surface, (TKE within the boils being approximately twice the TKE in ambient flow, with low frequency energy containing eddies having suppressed vertical fluctuations leaving the TKE redistributed and dominated by along and across-stream velocity variance), with their estimated TKE flux divergence; moving TKE produced at the BBL upward in CS. This closure is not fully complete, with the supposition that other TKE components could be important in the midwater; warranting further investigation.

Finding isotropic $^{-5}/_{3}$ inertial turbulence cascades at the surface was a surprising result (Talke et al., 2013), concluding that large-scale flow variations are anisotropic but that fluctuations with a frequency $\geq 1Hz$ / $\leq \mathcal{O}(1m)$ can still be considered isotropic. However despite these scales blocking the estimation of dissipation rates they can be estimated from the horizontal components at larger scales than those blocked in the vertical.

There have also been modelling efforts to describe these commonly occurring environmental bursting phenomena (Ikhennicheu et al., 2017; Omidyeganeh et al., 2011). The parameters

of boil morphology are not well constrained due to the large variation with observational situation, ranging from flume tank, stratified and fully mixed open channel flows in both oceans and rivers and with those of theoretical considerations.

1.4.2 Coherent Structures & TEC

There has been a recent surge in interest of CS and boils due to their effects on TEC devices. Analysts of wind turbine loading, such as Kelley et al. (2005), use the common metric of coherent turbulent kinetic energy (CTKE) defined as:

$$CTKE = \frac{1}{2}\sqrt{(u'w')^2 + (u'v')^2 + (v'w')^2} \tag{1.3}$$

which identifies peaks in $\mathbb{R}$ but with no temporal coherence. These authors supplement this with Wavelet analysis which allows time-frequency domain information of intermittent events, as also done in the works of Thomson et al. (2010) for oceanic flows. This technique has been applied with some success to analyse flows over dune beds by Salim et al. (2017) revealing intuitively a correlation between momentum and sediment flux and their contribution to the energy spectrum, finding that the transport mechanism for sediment flux relies on the production of momentum flux by CS, (they also provide a schematic of the sequence of turbulent bursting phenomena from BBL).

McCaffrey et al. (2015) utilises Acoustic Doppler Velocimeter (ADV) analysis of tidal flows with an interest in stresses on TEC devices, focusing on quantifying CS of $\mathcal{O}(10m)$, developing a coordinate-system invariant scalar magnitude of the anisotropy, which captures both shear stresses, normal stresses and strength of TKE.

They use this anisotropy magnitude, velocity structure functions (Webb, 1964) for timescale information, PDF's for intermittency and anisotropic nonlinear invariant maps based on the eigenvalues of the anisotropy tensor, such as those described in detail in Emory et al. (2014) for ABL studies, for the physical description of anisotropy, where for isotropic turbulence II = A = 0. They surmise that this single metric, A, is capable of characterising CS, particularly w.r.t. turbine loading and that turbulent stresses within CS are primarily one- or two-dimensional in contrast to isotropic three-dimensional turbulence but that at smaller scales, as found with other studies (those mentioned above and Thomson et al. (2012)), are isotropic. They also find that

simple PDF's are able to give similar information; both suggesting the strongest component of turbulence is aligned in the along-stream direction, but that this may be a 'bleeding' of residual tidal flow being categorised as turbulence. Vortex shedding from topography would produce two-dimensional turbulence, which is also observed in this study, giving an energy cascade with a slope of $^2/_3$, but they require high resolution surface measurements to confirm this.

Thiébaut et al. (2019) utilise an ADCP to study ambient turbulence in Alderney Race with a view to tidal energy assessment, noting that there are issues with the wider range of length and time scales in these flows, and that turbulent features of tidal flow are still poorly understood which is indicative of the difficulties (technical and theoretical) of acquiring and processing measurements of turbulent structures. They, among many other authors in the field (Bouferrouk et al., 2016; Garcia Novo et al., 2019; Gunawan et al., 2014; Hay et al., 2013; Lewis et al., 2019; MacEnri et al., 2013; McCaffrey et al., 2015; Milne et al., 2011; Mycek et al., 2014; Pieterse et al., 2017; Sentchev et al., 2020; Thomson et al., 2012, 2010) utilise transfer functions from the wind sector to study material fatigue and power generation alterations, namely the International Electrotechnical Commission's (IEC) standard metric of turbulence intensity (TI):

$$I = \frac{\sigma}{U} \tag{1.4}$$

Where U is the mean velocity and σ is the standard deviation to the mean velocity.

Milne et al. (2011) states that a lack of confidence in turbulent flow characterisation results in conservative estimates being employed by turbine designers and that non-homogeneous flow features on the scales of typical rotor diameters cannot always be studied accurately due to ADCP beam spread.

Recent modelling studies utilising LES include Mercier et al. (2019, 2021) and Ouro et al. (2019). Ouro et al. (2019) providing quantitative evidence of large-scale energetic turbulent structures induced by the seabed affecting instantaneous turbine performance and structural loading via bending moments. Mercier et al. (2019) produce λ_2 model visualisations of

CS over complex sea bottom morphology (seabed roughness, rocks, rifts, rapid changes of bathymetry) with vertical profiles of velocity and velocity variance giving good agreement with their in-situ ADCP measurements. Further study (Mercier et al., 2021) of this phenomena revealed high spatial variability of the TKE production and associated reduction in flow average velocity. These highly turbulent regions produce trails of vortices released from the seabed that, on intersection and aggregation with another vortex trail, generate a CS and subsequently a surface boil.

Further theoretical studies have been undertaken with DNS with Iyer et al. (2017) observing that independent of anisotropic energy containing eddies, the small-scale fluctuations recover isotropy quickly, and studies linked with experimental flume tanks where Ikhennicheu et al. (2017) analyse bathymetry influences on tidal stream site simulations and the formation of CS, finding that Kolk/Λ-vortices are formed from intermittency of the flow over obstacles (such as dunes) where the flow reattaches behind the obstacles inclined surface.

1.4.3 Methodology

This subsection aims to introduce coherent structures and boils and the measurement techniques used in the following papers in an illustrative manner.

Some background videos, if desired, as to what the instruments are trying to observe can be seen in the following short clips. This first link is a fantastic close up example of a boil caused by a coherent structure in a riverine context: [Riverine boil video, best viewed from 00 to 16 s]. This second video illustrates well the size boils can reach in a tidal strait: [Boils in Pentland Firth, North of Stroma. Best viewed from 33 to 53 s]. This last video illustrates the persistence of boil features to incoming surface waves, in this case bow waves from the vessel: [Boils at Corryvreckan, the strait North of Jura. Best viewed from 8 mins 03 s to 8 mins 23 s].

The life-cycle of a coherent structure from formation through to dissipation as a free-surface boil is illustrated in the schematic in Figure 1.1.

This study utilises a Nortek Signature 1000 ADCP and two PointGrey BlackFly high resolution cameras to capture coherent structures and boil morphology. The ADCP within the seabed frame, with attached Ethernet adaptor for land based control and the high resolution cameras

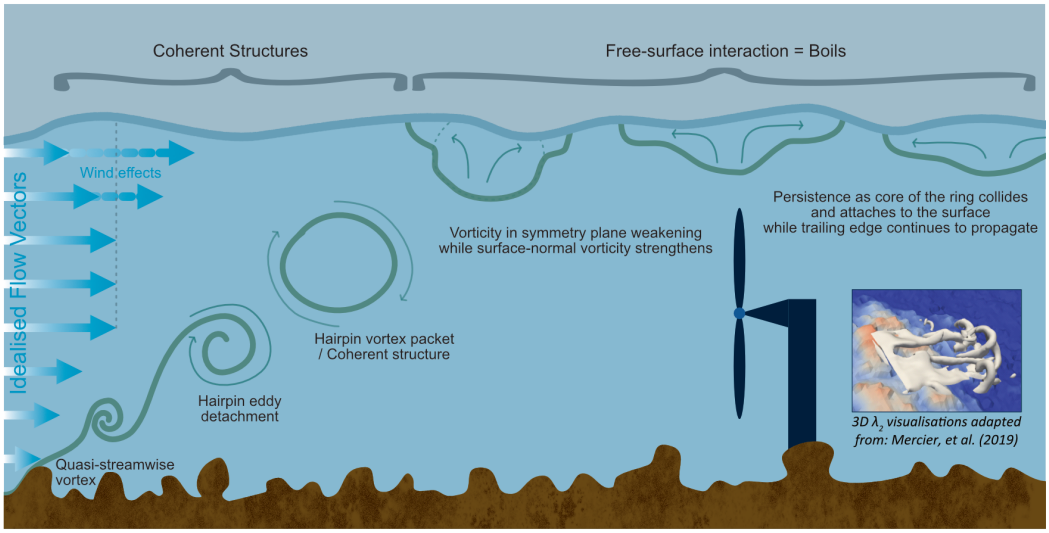

Figure 1.1 – Schematic illustrating the life-cycle of a coherent structure from generation at the sea bed to dissipation at the free-surface. Accompanied by an inlay figure from Mercier et al. (2019) showing a simulation of λ_2 isosurface plot of a 10 m wide turbulent coherent flow structure generated at bathymetric elevations.

are illustrated in Figure 1.2. All further details of instrumentation and configuration, capture scenarios and processing is detailed in the subsequent papers.

Figure 1.2 – Top Left: Image of the ADCP within the seabed frame, with attached Ethernet adaptor for land based control. Bottom right: Image of the high resolution cameras attached to the University Building.

Chapter 2

Characterising Surface Expressions of Turbulent Coherent Structures in a Tidally Energetic Channel.

The following chapter has been removed as it is to be submitted as "Characterising Surface Expressions of Turbulent Coherent Structures in a Tidally Energetic Channel" for publication in Ocean Science, European Geosciences Union.

Chapter 3

Turbulence and Coherent Structure Characterisation in a Tidally Energetic Channel.

The following chapter has been removed as it has been submitted as "Turbulence and Coherent Structure Characterisation in a Tidally Energetic Channel" for publication in Renewable Energy, Elsevier.

Chapter 4

Discussions & Conclusions

The manuscripts presented here have developed and tested methodologies for characterisation of coherent structures at the scales likely to compromise the structural integrity of tidal energy infrastructure and its operational performance, namely the intermediate scales between the production of TKE and its subsequent small-scale dissipation. Outside of the TEC industry CS characterisation can be useful to elucidate information about transportation of sediments, pollution, and phytoplankton blooms (Garaboa-Paz et al., 2015; Knapp et al., 2020; Lindemann et al., 2017; Nimmo Smith et al., 1999; Salim et al., 2017).

Chapter 2 obtained the free-surface signature of CS with methodology derived using geo-rectified images from high resolution cameras to delineate boil boundaries; giving size, growth rate, circular expansion speed, displacement speed and advection velocity. This information has then been correlated with beam-averaged Janus beams, and in Chapter 3 with high resolution vertical beam parameters, from a bed mounted ADCP to ascertain CS metrics within the water column.

In chapter 2 free-surface boil parameters were assessed through both the semi-diurnal and lunar tidal cycles finding that boil occurrence is greatest around high water and evident on the flood tide from up to 4 hours before high. No boils were observed above the ADCP on the ebbing tide, suggesting that boil and thus CS occurrence is flow-direction and location dependent which, at the time of submission, was thought to be due to seabed morphology or boundary layer structure. The former hypothesis is supported in recent modelling works by Mercier et al. (2019, 2021) and Ouro et al. (2019) who find that CS are induced by complex seabed morphology. Mercier et al. (2021) find that vortices released from the seabed generate CS from intersection and aggregation with other vortex trails. Taken together with the findings in this thesis, this suggests significant spatial variability and localised flow changes affect CS

and boil occurrence, which further suggests that site specific analysis of tidal stream turbine locations is warranted.

The boil dimensions obtained in chapter 2 are consistent with literature values, scaling with water depth (Nimmo Smith et al., 1999; Thorpe et al., 2008). Moreover this thesis finds that boil extents at the free-surface are dissimilar to that of coherent structures within the flow, which is also consistent with the findings of Nimmo Smith et al. (1999) and Thorpe et al. (2008). This supports the hypothesis that it is not possible to commute boil to CS parameter space.

Correlations between boil occurrence and tidally averaged flow components were obtained in chapter 2, showing boils occurred when cross-channel and vertical flow components were maximal, with the highest correlations found with the downward component of vertical flow. This is consistent with the works of Adrian et al. (2012) and Sukhodolov et al. (2011) and illustrated well in Sukhodolov et al. (2011, Figure 4) shown here:

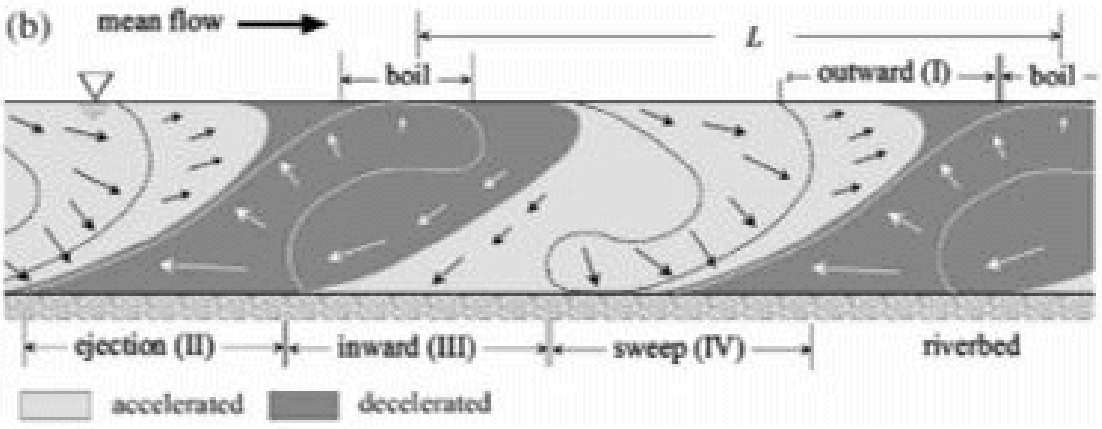

Figure 4.1 – Schematic representation of large-scale turbulence in open-channel flow (Sukhodolov et al., 2011, Figure 4)

Chapter 3 analysed metrics utilising both high frequency single vertical beam analysis techniques and that of the across beams variance method.

The findings suggest that small-scale turbulent dissipation does not necessarily correlate with CS incidence and so measurement of profiles of epsilon provide a poor predictor for the incidence of CS. Fast Fourier transforms were found to be a tool with which CS structures can be elucidated, but without time-localised identification as the transform is integrated over

a 30-minute tidal slice. Taking insights from other studies (Kelley et al., 2000; Keylock, 2007; Salim et al., 2017; Thomson et al., 2010), wavelets facilitate extraction of time-localised non-sinusoidal periodic signals from velocity time series. Chapter 3 extends simple wavelets by utilising a wavelet element model (Lilly, 2017), which facilitates significance and region of influence element analysis.

Applying this model to the vertical velocity datasets during periods of boil activity, CS lengthscales of the most powerful features in the analysis period were ascertained to be 16.9 $\pm$ 11.2 m with a median of 13.2 m, which lies within the tolerance of the lengthscales of interest to the tidal energy industry with tidal turbine rotor diameters and blade cord lengths commonly quoted to be $\mathscr{O}10$ m and $\mathscr{O}1$ m respectively.

When coherent structures are present in the water column, chapter 3 finds that the usage of the variance method to ascertain TKE metrics is flawed due to covariance being present between the beams as CS lengthscales match those of the beam spread. This leads to significant bias in estimates of TI, Reynolds stresses and TKE production. Thomson et al. (2012) concur with this finding finishing their study with comments on the limitations of ADCP's due to the beam spread when utilising variance methods such as turbulent intensity and they comment on the need to further constrain the general structure of such eddies at tidal energy sites. This has wide implications for calculation of turbulence parameters via the variance method when CS are present in the water column.

In summary

- Site specific analysis of tidal stream turbine locations is warranted due to spatial and flow variability in CS formation.
- CS and boil dimensions scale with water depth.
- It is not possible to commute boil dimension to CS dimension parameter space using these methods.
- Tidally averaged downward orientation of vertical velocity components is a good indicator of the presence of boils at the surface.
- Measurements of turbulent dissipation are not a good indicator of CS incidence.
- CS lengthscales were found to be within the tolerance of lengthscales of interest to the tidal energy industry

- When coherent structures are ubiquitous covariance is present between ADCP beams, attributed to CS lengthscales being of the same order as that of the beam spread, leading to significant bias in estimates of TI, Reynolds stresses and TKE production via the variance method.

4.0.1 Further Work

This work uncovers the variability of CS at the MTO both synoptically and spatially, which implies the need for site specific characterisation at planned turbine locations with the metrics evaluated here. Understanding CS structure, size and residence time in the water column can be useful for the placement of tidal turbines and their operational windows. Such site characterisation could reveal trends in properties and features that bring about similar outcomes, honing our understanding of site specific restraints, engineering constraints and optimal power windows.

At the current MTO location, an algorithm could be written to capture the boil extents from the camera images, saving labour time and increasing the number of detection's measured. This could be parameterised to not simply detect and measure extents, but also to collect parameters such as advection through the image space and shape transformation at the surface. This would allow greater confidence in the consistency of the measurements with increased statistics.

In modelling studies, seabed morphology is known to alter the hydrodynamic characteristics of the flow (Mercier et al., 2021; Ouro et al., 2019) and this thesis supports that hypothesis with synoptic variability of CS as flow direction upstream to the ADCP has different bed morphology at different stages of the tidal cycle. Bathymetry data collected at this site (Walker-Springett, 2020) could be scrutinised to provide an element lengthscale (Adrian et al., 2012; Guala et al., 2012) of the dunes found upstream of the ADCP when CS are present during the flooding tide. This could elucidate to seabed structure influence on coherent structure size, frequency and amalgamation and if analysed with boundary layer information obtained from the ADCP (Hay et al., 2013), could tease out the possible contrasting influences of these features on CS morphology .

Chapter 3 utilises a wavelet element model to advance our interpretation of CS morphology captured with data from one tidal slice. The data suggests that there is a periodic repetition

of CS events, consistent with literature (Heathershaw, 1974). Increasing the number of tidal cycles scrutinised would be beneficial in iteration of datasets to deepen our understanding of CS movement in the water column, advection speeds, CS size changes inferred from the transform period, and signal amplitude variations over depth hinting at spatial energy variation within the CS with possible links from lengthscale to depthscale.

Identification of metrics utilising ADCP's to improve our understanding of anisotropy employing methods other than the variance method would be advantageous in environments that contain CS. This could inform possible bias in Structure Function parameterisations from anisotropy and shear. This could then lead on to greater scrutiny of energy balances within tidal races.

Appendix A

An Introduction to Turbulence

A turbulent flow occurs in a high Reynolds number environment, with Reynolds number (Re) being defined as the ratio of inertial to viscous forcing;

$$R_e = \frac{UL}{\nu} \tag{A.1}$$

where U is the flow velocity, L is a length scale, and ν is kinematic viscosity.

Turbulent flows cannot be precisely defined, they are by their nature chaotic, but the characteristics of turbulence can be described as being or displaying: irregular/disordered, diffusivity/mixing, vorticity/rotational 3D fluctuations, dissipative/needing a continuous supply of energy, continuum phenomena (small scales being far larger than molecular length scales) (Tennekes et al., 1972).

Of useful insight to the basics of fluid mechanics, are the 1960's shorts produced by the National Committee for Fluid Dynamics Films, some of which have been made available on the web by MIT here: http://web.mit.edu/hml/ncfmf.html. It is useful here to describe the video therein of turbulent flows, as this summaries succinctly the pathway of turbulent processes.

Turbulence causes a mixing of momentum which homogenises the flow by increasing the effects of molecular diffusion from inhomogeneities by way of vortex streaks, described below. The 'wall' or boundary is a sink of momentum, increasing boundary roughness increases the ratio of turbulent to mean flow speeds, the momentum towards the wall on average being greater than that moving away from the wall with cross stream velocities mixing the flow properties, thus turbulence is able to carry fluid properties; known as turbulent transport.

Turbulence displays 'similarity', whereby motions display similar structure and can be defined by the length scales of motion and quantified by the energy dissipated from simple principles applied to flows with different Re:

$$\varepsilon = \nu\overline{\gamma^2} \tag{A.2}$$

where $\overline{\gamma^2}$ is the mean squared strain rate, which represents the rate at which energy is transferred from the mean flow to TKE, which is balanced by ε; the the rate at which this TKE is dissipated to heat. The strain pulls out 'blobs' of properties into elongated forms (vortex streaks) increasing interfacial area and property gradients that aid molecular diffusion. This simple understanding leads to:

$$\frac{\varepsilon}{U^2} = \frac{\nu}{L^2} \tag{A.3}$$

which is the dimensional argument that states that if energy is dissipated and speed of two flows are the same while having different viscosities, then the lengthscale of the turbulence must be different, i.e. differences in R_e are not apparent in large scale turbulence but in the small scales of motion.

The onset of turbulence depends on a growth of perturbations from an instability. These instabilities, in mathematical terms, are interactions between viscous and nonlinear inertia terms in the equations of motion; in this case the Navier-Stokes (N-S) equations. Initial and boundary conditions set the characteristics of common turbulent parameters.

Now, turbulence by definition is a continuum and as such the N-S equation can be derived from Cauchy Momentum equations in an inertial frame of reference, (Kundu et al., 2002), for its incompressible form the continuity equation is $\frac{\partial U_i}{\partial x_i} = 0$, giving the N-S momentum equation in tensor form for average velocity component U_i:

$$\frac{\partial \rho U_i}{\partial t} + \frac{\partial}{\partial x_j}(\rho U_i U_j) + \frac{\partial p}{\partial x_i} - \frac{\partial}{\partial x_j}\mu\left(\frac{\partial U_i}{\partial x_j} + \frac{\partial U_j}{\partial x_i}\right) = \rho\Gamma_i \tag{A.4}$$

where Γ is the body force or external source and μ is the viscosity. This equation states that the momentum change of a fluid element is driven by three forces, gradients of the pressure, divergence of a friction tensor (diffusion) and long range forces, (Schmidt, 2015).

In non-tensor notation, dividing through by density and substituting with the kinematic viscosity, $\nu = \frac{\mu}{\rho_0}$:

$$\overbrace{\underbrace{\frac{\partial \mathbf{u}}{\partial t}}_{\text{Variation}} + \underbrace{(\mathbf{u}.\nabla)\mathbf{u}}_{\text{Advection}}}^{\text{Inertia (per volume)}} + \overbrace{\underbrace{\frac{1}{\rho}\nabla p}_{\text{Internal Source}} - \underbrace{\nu\nabla^2\mathbf{u}}_{\text{Diffusion}}}^{\text{Divergence of stress}} = \underbrace{\Gamma}_{\text{External Source/Body Force}} \tag{A.5}$$

where $\mathbf{u}(\mathbf{x},t)$ from an Eulerian viewpoint, (Schmidt, 2015).

Comparing this to the Cauchy Momentum Equation one can observe the meanings of these terms, as shown with the brackets.

Now, if we take equation A.4 and perform a Reynolds decomposition, whereby we describe the flows with a time averaged and fluctuating component such that: $U_i = \overline{u_i} + u_i'$, defining a suitable average, (space, time, or ensemble (Stewart, 1969) constrained by the demand of quasi-stationarity within the averaging period while being long enough to give statistically reliable estimates), the resulting equation defines the N-S equation in a form that gives the Reynolds stress tensor – which contains the nonlinear terms giving rise to turbulence:

As earlier, the continuity equation is: $\frac{\partial \overline{u_i}}{\partial x_i} = 0$, leaving:

$$\rho\frac{\partial \overline{u}_i}{\partial t} + \rho\frac{\partial}{\partial x_j}(\overline{u}_i\overline{u}_j) = -\frac{\partial \overline{p}}{\partial x_i} + \frac{\partial}{\partial x_j}(2\mu S_{ij} - \rho\overline{u_i'u_j'}) + \rho\Gamma_i \tag{A.6}$$

where

$$S_{ij} = \frac{1}{2}\left(\frac{\partial \overline{u}_i}{\partial x_j} + \frac{\partial \overline{u}_j}{\partial x_i}\right) \tag{A.7}$$

is the mean rate of strain tensor or viscous stress, and the additional stress $\tau_{ij} = -\rho\overline{u_i'u_j'}$ is known as the Reynolds Stress tensor, $\mathbb{R}$ (Kundu et al., 2002), the divergence of which is the force density on the fluid due to the turbulent fluctuations and is much larger than the viscous

contribution when not near the boundaries. It should be noted that these are not actually additional 'stresses', but are actually additional momentum fluxes from the turbulent motions interpreted as effective stresses. (Brennen, 2006)

$\mathbb{R}$, is a symmetric tensor with its diagonal components being normal stresses and its off-diagonal components shear stresses which vanish if the turbulent fluctuations are completely isotropic, i.e. $\overline{u'^2} = \overline{v'^2} = \overline{w'^2}$

$$\mathbb{R} = \begin{bmatrix} -\rho\overline{u'^2} & -\rho\overline{u'v'} & -\rho\overline{u'w'} \\ -\rho\overline{u'v'} & -\rho\overline{v'^2} & -\rho\overline{v'w'} \\ -\rho\overline{u'w'} & -\rho\overline{v'w'} & -\rho\overline{w'^2} \end{bmatrix} \tag{A.8}$$

As stated, the onset of turbulence depends on a growth of perturbations from instabilities which are interactions between viscous and nonlinear inertia terms in the equations of motion, as such it is at this time not possible to make accurate quantitative predictions and statistical studies generate unknowns which lead to what is called the closure problem of turbulence theory (Tennekes et al., 1972) and one has to make assumptions to evaluate perturbation schemes.

These local assumptions, which state that large and small scale turbulent structures of motion are independent of each other and the mean deformation rate (Kolmogorov, 1941, 1942), are the foundation of the majority of measurement and modelling techniques. The rate of mixing is inferred by the transfer of turbulent kinetic energy (TKE) from production at the large scale overturning motions (which can be anisotropic) down to smaller isotropic eddies and ultimately dissipation through viscosity (Richardson, 1922) via the inertial subrange, with the inertial subrange and the dissipation range collectively known as the universal equilibrium range. This theory is known as the local equilibrium hypothesis and is explained well in Tennekes et al. (1972):

> "Since small-scale motions tend to have small time scales, one may assume that these motions are statistically independent of the relatively slow large-scale turbulence and of the mean flow. If this assumption makes sense, the small-scale motion should depend only on the rate at which it is supplied with energy by the large-scale motion and on the kinematic viscosity. It is fair to assume that the rate of energy supply should be equal to the rate of dissipation, because the net rate of change of small-scale energy is related to

the time scale of the flow as a whole. The net rate of change, therefore, should be small compared to the rate at which energy is dissipated. This is the basis for what is called Kolmogorov's universal equilibrium theory of the small-scale structure."

This hypothesis gives the basis of the Taylor dissipation law (Taylor, 1935) as first derived by (Kolmogorov, 1941) and subsequently written down by Taylor, as such it is known as the Taylor-Kolmogorov dissipation law for isotropic turbulence and can be written as:

$$\varepsilon = 15\nu \left(\frac{\overline{U^2}}{L^2} \right) \tag{A.9}$$

where L is the average size of the smallest eddies, $\overline{U^2}$ is the mean square variation in one component of velocity and ε is the rate of dissipation of energy. Which is true for high Reynolds number flows where the small scale motions are statistically isotropic and has been verified experimentally (Corrsin, 1958; Taylor, 1935; Townsend, 1976).

This requires simultaneous measurements of all components of velocity at multiple points, which can be experimentally challenging, thus it is common to measure one of these velocity components at one point over a period of time, converting time signals to spatial signals using $x = Ut$, with U being the time averaged velocity. This is commonly referred to as Taylor's hypothesis of frozen turbulence, which is only valid for $u'/U \ll 1$, which assumes that the turbulent fluctuations at a point are caused by the advection of a frozen field past a point, (Kundu et al., 2002).

The scale of the smallest eddies present in the flow is the Kolmogorov microscale ($\eta = (\nu^3/\varepsilon)^{1/4}$), it is worth noting that this is the scale at which the energy is dissipated.

For the inertial subrange, the one-dimensional u spectrum can be expressed as, according to Kolmogorov's law:

$$F_u(k_1) = \alpha_1 \varepsilon^{2/3} k_1^{-5/3} \tag{A.10}$$

where k_1 is the wavenumber in the x direction ($k_1 = 2\pi n/U$, by Taylor's hypothesis), and α, is a universal constant estimated from various experiments to be approximately 0.5.

This theory assumes that turbulence at high Reynolds numbers is completely random and isotropic, but in practice a boundary layers mean strain rate in a turbulent sheared flow can cause anisotropy, particularly at the large scales. However it is often argued that the process of transferring energy down through the spectral scales will destroy this orientation, leading to structure independent of orientation effects induced by this mean shear at the small scale, and thus local isotropy can still be justified; this should hold in regions where the local transfer time is shorter than that of the gross shear strain (Corrsin, 1958).

It is informative here to define the similarity theory which leads to some commonly used terms, such as the Obukhov lengthscale, friction velocity, roughness lengthscale and the law of the wall, all commonly used parameters in describing turbulent boundary layers (Foken, 2006), which is the layer next to the wall consisting of a viscous sublayer, a buffer layer, (collectively known as the roughness sublayer), and a logarithmic boundary layer, before the flow transitions to the free stream laminar flow.

The Obukhov length scale, derived from the Monin-Obukhov similarity theory; a dimensional analysis using the Buckingham π-theorem of the TKE equations and the ratio of the buoyancy and shearing effects, is one of a 'dynamical sublayer' which describes turbulence above the roughness sublayer, where stratification influences are negligible (Monin et al., 1975a,b) and is defined as:

$$L = -\frac{u_*^3}{\kappa(\frac{g}{T_0})(\frac{Q}{C_p\rho})} \tag{A.11}$$

with

$$\overline{w'T'} = \frac{Q}{C_p\rho} = const, \tag{A.12}$$

$$-\rho\overline{u'w'} = \tau = const, \tag{A.13}$$

$$u_* = \sqrt{\frac{\tau}{\rho}} \tag{A.14}$$

where u_* is a friction or shearing velocity, κ is the von Kármán constant, g is the gravitational acceleration, T_0 is mean temperature, Q is the kinematic heat flux, c_p the specific heat, ρ is the density, T' is the fluctuating temperature, w' is the fluctuating vertical velocity and τ is the turbulent shear stress. (It should be noted that the Monin-Obukhov similarity theory breaks down within roughness sublayers such as those within canopies). These scales are important as they are used within the text from a dimensional analysis viewpoint of surface-layer flow properties via dimensionless universal functions of z/L, where z is the height above the boundary and positive (negative) values indicating stable (unstable) values, approaching 0 in the limit of neutral stratification.

If the turbulent motion is independent of kinematic viscosity, on dimensional grounds the mean velocity shear dU/dz can be given by:

$$\frac{dU}{dz} = \frac{u_*}{\kappa z} \tag{A.15}$$

On integration this leads to:

$$U(z) = \frac{u_*}{\kappa}[ln(z) - ln(z_0)] \tag{A.16}$$

with z_0 being the roughness length scale which depends on the size of the boundary roughness. u_* can be estimated from measurements at two distances, z_1 and z_2:

$$u_* = \frac{\kappa[U(z_1) - U(z_2)]}{ln(z_1/z_2)} \tag{A.17}$$

Now, balancing terms implies that approximately:

$$\varepsilon = \left(\frac{\tau}{\rho_0}\right)\frac{dU}{dz} \tag{A.18}$$

so equation A.15 and equations A.18 gives:

$$\varepsilon = \frac{u_*^3}{\kappa z} \tag{A.19}$$

and implies that the size of the dominant turbulent eddies, l, increases in proportion to z. These definitions are commonly known as the 'Law of the Wall' (Bradshaw et al., 1995; Karman, 1930).

References

Adrian, R. J. and Ivan Marusic (2012). 'Coherent structures in flow over hydraulic engineering surfaces'. In: *Journal of Hydraulic Research* 50.5, pp. 451–464 (p. 25, 27).

Antonia, R. A. and R. E. Luxton (1972). 'The response of a turbulent boundary layer to a step change in surface roughness. Part 2. Rough-to-smooth'. In: *Journal of Fluid Mechanics* 53.4, pp. 737–757 (p. 11).

Bakewell, H. P. (1966). 'Ph.D Dissertation'. PhD thesis (p. 7).

Baylyl, B. J. and S. A. Orszag (1988). 'Instability Mechanisms in Shear-Flow Transition'. In: *Ann. Rev. Fluid Mech* 20, pp. 359–91 (p. 12).

Black, T. J. (1968). 'A New Model of the Shear Stress Mechanism in Wall Turbulence'. In: *AIAA* 68-42 (p. 7).

Bouferrouk, A, Jonathan P. Hardwick, Antonella M. Colucci and Lars Johanning (2016). 'Quantifying turbulence from field measurements at a mixed low tidal energy site'. In: *Renewable Energy* 87, pp. 478–492 (p. 18).

Bowden, K. F. (1962). 'Measurements of Turbulence near the Sea Bed in a Tidal Current'. In: *Journal of Geophysical Research* 67.8, pp. 3181–3186 (p. 13).

Bowden, K. F. and L. A. Fairbairn (1956). 'Measurements of Turbulent Fluctuations and Reynolds Stresses in a Tidal Current'. In: *Proceedings of the Royal Society A: Mathematical, Physical and Engineering Sciences* 237, pp. 422–438 (p. 12).

Bradshaw, P. (1967). ''Inactive' motion and pressure fluctuations in turbulent boundary layers'. In: *J. Fluid Mech.* 30.2, pp. 241–253 (p. 7).

Bradshaw, P. and G. P. Huang (1995). 'The Law of the Wall in Turbulent Flow'. In: *Proceedings: Mathematical and Physical Sciences* 541.1941, pp. 165–188 (p. 36).

Brennen, C. E. (2006). *An Internet Book on Fluid Dynamics* (p. 32).

Chickadel, C. C., A. R. Horner-Devine, S. A. Talke and A. T. Jessup (2009). 'Vertical boil propagation from a submerged estuarine sill'. In: *Geophysical Research Letters* 36.10, pp. 2–7 (p. 15, 16).

Chickadel, C. C., S. A. Talke, A. R. Horner-Devine and A. T. Jessup (2011). 'Infrared-based measurements of velocity, turbulent kinetic energy, and dissipation at the water surface in a tidal river'. In: *IEEE Geoscience and Remote Sensing Letters* 8.5, pp. 849–853 (p. 15, 16).

Corino, E.R. and R. S. Brodkey (1969). 'A visualization of the wall region in turbulent flow'. In: *Journal of Fluid Mechanics* 37, pp. 1–30 (p. 6–8, 12, 14).

Corrsin, S. (1958). 'Local Isotropy in Turbulent Shear Flow'. In: *NACA RM* 58B11.April, pp. 1–32 (p. 33, 34).

Corrsin, S. and A. L. Kistler (1955). *Free stream boundaries of turbulent shear flows*. Tech. rep. Johns Hopkins University (p. 11).

Day, A. H., A. Babarit, A. Fontaine, Y. P. He, M. Kraskowski, M. Murai, I. Penesis, F. Salvatore and H. K. Shin (2015). 'Hydrodynamic modelling of marine renewable energy devices: A state of the art review'. In: *Ocean Engineering* 108, pp. 46–69 (p. 4).

Dewey, R. K. and S. Stringer (2007). 'Reynolds Stresses and Turbulent Kinetic Energy Estimates from Various ADCP Beam Configurations : Theory'. In: *Journal of Physical Oceanography* July 2015, pp. 1–35 (p. 5).

Einstein, H. A. and H. Li (1955). *Heat Transfer and Fluid Mechanics*. Tech. rep. Inst. Univ. California, Los Angeles (p. 7).

Emory, M. and G. Iaccarino (2014). 'Visualizing turbulence anisotropy in the spatial domain with componentality contours'. In: *Center of Turbulence Research, Annual Research Briefs*, pp. 123–138 (p. 17).

Favre, A., J. Gaviglio and R. Dumas (1967). 'Structure of velocity space-time correlations in a boundary layer'. In: *Physics of Fluids* 10.9 (p. 8).

Ferrari, C. (1959). *Wall turbulence*. Tech. rep. NASA Re, 2–8–59W (p. 7).

Fiedler, H. and M. R. Head (1966). 'Intermittency measurements in the turbulent boundary layer'. In: *Journal of Fluid Mechanics* 25.4, pp. 719–735 (p. 8).

Foken, T. (2006). '50 years of the Monin-Obukhov similarity theory'. In: *Boundary-Layer Meteorology* 119.3, pp. 431–447 (p. 34).

– (2008). 'The Energy Balance Closure Problem : An Overview'. In: *Ecological Applications* 18.6, pp. 1351–1367 (p. 9).

Gao, W., R. H. Shaw and K. T. Paw U (1989). 'Observation of organized structure in turbulent flow within and above a forest canopy'. In: *Boundary-Layer Meteorology* 47.1-4, pp. 349–377 (p. 11).

Garaboa-Paz, Daniel, Jorge Eiras-Barca, Florian Huhn and Vicente Peérez-Mũnuzuri (2015). 'Lagrangian coherent structures along atmospheric rivers'. In: *Chaos* 25.6 (p. 24).

Garcia Novo, Patxi, Yusaku Kyozuka and Maria Jose Ginzo Villamayor (2019). 'Evaluation of turbulence-related high-frequency tidal current velocity fluctuation'. In: *Renewable Energy* 139, pp. 313–325 (p. 18).

Gordon, C .M. and C. F. Dohne (1973). 'Some Observations of Turbulent Flow in a Tidal Estuary'. In: *J. Geophys. Res.* 78.12, pp. 1971–1978 (p. 12).

Grant, H. L. (1957). 'The large eddies of Turbulent Motion'. In: *J. Fluid. Mech. 4,* 4, pp. 149–190 (p. 7).

Grass, A. J. (1971). 'Structural features of turbulent flow over smooth and rough boundaries.pdf'. In: *Journal of Fluid Mechanics* 50.2, pp. 233–255 (p. 10).

Guala, Michele, Christopher D. Tomkins, Kenneth T. Christensen and R. J. Adrian (2012). 'Vortex organization in a turbulent boundary layer overlying sparse roughness elements'. In: *Journal of Hydraulic Research* 50.5, pp. 465–481 (p. 27).

Gunawan, Budi, Vincent S. Neary and Jonathan Colby (2014). 'Tidal energy site resource assessment in the East River tidal strait, near Roosevelt Island, New York, New York'. In: *Renewable Energy* 71, pp. 509–517 (p. 18).

Hardisty, J. (2008). 'Power Intermittency, Redundancy and Tidal Phasing around the United Kingdom'. In: *The Geographical Journal* 174.1, pp. 76–84 (p. 2).

Haugen, D. A., J. C. Kaimal and E. F. Bradley (1971). 'An experimental study of Reynolds stress and heat flux in the atmospheric surface layer'. In: *Quarterly Journal of the Royal Meteorological Society* 097.412, pp. 168–180 (p. 9).

Hay, Alex E., J McMillan, Richard Cheel and Douglas J. Schillinger (2013). 'Turbulence and Drag in a High Reynolds Number Tidal Passage Targetted for In-Stream Tidal Power'. In: *Oceans 2013 San DIego*, pp. 1–10 (p. 18, 27).

Heathershaw, A. D. (1974). '"Bursting" phenomena in the sea'. In: *Nature* 248.5447, pp. 394–395 (p. 12, 14, 28).

– (1979). 'Turbulent Structure of the Bottom Boundary-Layer in a Tidal Current'. In: *Geophysical Journal of the Royal Astronomical Society* 58.2, pp. 395–430 (p. 5, 12, 13).

Ikhennicheu, M. and P. Druault (2017). 'An experimental study of bathymetry influence on turbulence at a tidal stream site'. In: *EWTEC*, pp. 1–10 (p. 16, 19).

Iyer, K. P., F. Bonaccorso, L. Biferale and F. Toschi (2017). 'Multiscale anisotropic fluctuations in sheared turbulence with multiple states'. In: *Physical Review Fluids* 2.5, pp. 1–6. arXiv: 1707.00778 (p. 19).

Izumi, Y. (1971). *Kansas 1968 Field Program Data Report*. Tech. rep. Bedford, Mass.: Air Force Cambridge Research Laboratories (p. 9).

Johns, B. (1969). 'Some Consequences of an Inertia of Turbulence in a Tidal Estuary'. In: *Geophysical Journal International* 18.1, pp. 65–72 (p. 13).

Kaimal, J. C., J. C. Wyngaard, Y. Izumi and O. R. Coté (1972). 'Spectral characteristics of surface-layer turbulence'. In: *Quarterly Journal of the Royal Meteorological Society* 98.417, pp. 563–589 (p. 9, 13).

Karman, T. von (1930). 'Mechanische Ähnlichkeit und Turbulenz [Mechanical similarity and turbulence]'. In: *Nachrichten von der Gesellschaft der Wissenschaften zu Göttingen Mathematisch-physikalische Klasse* (p. 36).

Kelley, N. D., B. J. Jonkman, J. T. Bialasiewicz, G. N. Scott and L. S. Redmond (2005). 'The Impact of Coherent Turbulence on Wind Turbine Aeroelastic Response and Its Simulation'. In: *American Wind Energy Association WindPower 2005 Conference and Exhibition*, p. 17 (p. 3, 17).

Kelley, N. D., R. M. Osgood, J. .T. T. Bialasiewicz and A. Jakubowski (2000). 'Using Time-Frequency and Wavelet Analysis to Assess Turbulence/Rotor Interactions'. In: *American Institute of Aeronautics and Astronautics* 3.November 1999, pp. 121–134 (p. 2, 26).

Keylock, C. J. (2007). 'The visualization of turbulence data using a wavelet- based method'. In: *Earth Surface Processes and Landforms* 32, pp. 637–647 (p. 26).

Kim, H. T., S. J. Kline and W. C. Reynolds (1971). 'The production of turbulence near a smooth wall in a turbulent boundary layer'. In: *Journal of Fluid Mechanics* 50.1, pp. 133–160 (p. 8).

Kistler, A. L. (1962). 'Méchanique de la Turbulence'. In: *Editions du Centre National de la Recherche Scientifique*, p. 287 (p. 7).

Kline, S. J., W. C. Reynolds, F. A. Schraub and P. W. Runstadler (1967). 'The structure of turbulent boundary layers'. In: *Journal of Fluid Mechanics* 30.4, pp. 741–773 (p. 7, 8).

Knapp, Abigail S. and Adam M. Milewski (2020). 'Spatiotemporal relationships of phytoplankton blooms, drought, and rainstorms in freshwater reservoirs'. In: *Water (Switzerland)* 12.2, pp. 16–18 (p. 24).

Kolmogorov, A.N. (1941). 'The Local Structure of Turbulence in Incompressible Viscous Fluid for Very Large Reynolds' Numbers'. In: *Doklady Akademiia Nauk SSSR* 30, pp. 301–305 (p. 32, 33).

– (1942). 'Equations of turbulent motion in an incompressible fluid'. In: *Izv. Akad. Nauk SSSR* 6.1-2, pp. 56–58 (p. 32).

Kovasznay, L. S. G. (1970). 'The turbulent boundary layer'. In: *Ann. Rev. Fluid Mech.* (p. 8, 11).

Kumar, S., R. Gupta and S. Banerjee (1998). 'An experimental investigation of the characteristics of free-surface turbulence in channel flow'. In: *Physics of Fluids* 10.2, pp. 437–456 (p. 14).

Kundu, P. K. and I. M. Cohen (2002). *Fluid Mechanics*. second, p. 766 (p. 30, 31, 33).

Landahl, M. (1967). 'Wave-Guide Model for Turbulent Shear Flow'. In: *Physics of Fluids* 10.9, S310 (p. 7).

Lewis, Matt, James McNaughton, Concha Márquez-Dominguez, Grazia Todeschini, Michael Togneri, Ian Masters, Matthew Allmark, Tim Stallard, Simon Neill, Alice Goward-Brown and P. E. Robins (2019). 'Power variability of tidal-stream energy and implications for electricity supply'. In: *Energy* 183, pp. 1061–1074 (p. 18).

Lilly, J. M. (2017). 'Element analysis: a wavelet-based method for analyzing time-localized events in noisy time series'. In: *Proceedings of the Royal Society A: Mathematical, Physical and Engineering Sciences* 473.20160776 (p. 26).

Lindemann, Christian, Andre Visser and Patrizio Mariani (2017). 'Dynamics of phytoplankton blooms in turbulent vortex cells'. In: *Journal of the Royal Society Interface* 14.136 (p. 24).

Lohrmann, Atle, Bruce Hackett and Lars Petter Røed (1990). 'High Resolution Measurements of Turbulence, Velocity and Stress Using a Pulse-to-Pulse Coherent Sonar'. In: *Journal of Atmospheric and Oceanic Technology* 7.1, pp. 19–37 (p. 5, 6).

Lu, Youyu and R G Lueck (1999). 'Using a Broadband ADCP in a Tidal Channel. Part I: Mean Flow and Shear'. In: *Journal of Atmospheric and Oceanic Technology* 16, pp. 1556–1567 (p. 5).

Lucas, N. S., J. H. Simpson, T. P. Rippeth and Christopher P. Old (2014). 'Measuring turbulent dissipation using a tethered ADCP'. In: *Journal of Atmospheric and Oceanic Technology* 31.8, pp. 1826–1837 (p. 5).

MacEnri, J., M. Reed and T. Thiringer (2013). 'Influence of tidal parameters on SeaGen flicker performance'. In: *Philosophical Transactions of the Royal Society A: Mathematical, Physical and Engineering Sciences* 371.1985 (p. 18).

Malkus, W. V. R. (1956). 'Outline of a theory of turbulent shear flow'. In: *Journal of Fluid Mechanics* 1.5, pp. 521–539 (p. 7).

McCaffrey, K. (2018). 'Characterizing Turbulence at a Prospective Tidal Energy Site: Observational Data Analysis'. In: *Ocean Seminar* (p. 3).

McCaffrey, K., B. Fox-Kemper, P. E. Hamlington and Jim Thomson (2015). 'Characterization of turbulence anisotropy, coherence, and intermittency at a prospective tidal energy site: Observational data analysis'. In: *Renewable Energy* 76, pp. 441–453 (p. 17, 18).

Mercier, P., Mikaël Grondeau, Sylvain Guillou, Jérôme Thiébot and Emmanuel Poizot (2019). 'Numerical study of the turbulent eddies generated by the seabed roughness. Case study at a tidal power site.' In: *Applied Ocean Research* 2016 (p. 18, 20, 24).

Mercier, P. and Guillou S Sylvain (2021). 'The impact of the seabed morphology on turbulence generation in a strong tidal stream'. In: *Physics of Fluids* 33.May (p. 18, 19, 24, 27).

Milne, I. A., A. H. Day, R. N. Sharma and R. G.J. J Flay (2016). 'The characterisation of the hydrodynamic loads on tidal turbines due to turbulence'. In: *Renewable and Sustainable Energy Reviews* 56, pp. 851–864 (p. 4).

Milne, I. A., Rajnish N Sharma, Richard G J Flay and Simon Bickerton (2011). 'Characteristics of the onset flow turbulence at a tidal-stream power site'. In: *EWTEC 2011 Proceedings* (p. 18).

Mitchell, J. E. and T. J. Hanratty (1966). 'A study of turbulence at a wall using an electrochemical wall shear-stress meter'. In: *J. Fluid Mech.* 26.199 (p. 7).

Monin, A. S. and A. M. Yaglom (1975a). *Statistical Fluid Mechanics: Mechanics of Turbulence, Vol. 1*. Cambridge, London: MIT Press, p. 874 (p. 34).

– (1975b). *Statistical Fluid Mechanics: Mechanics of Turbulence, Vol. 2*. Cambridge, London: MIT Press, p. 874 (p. 34).

Mycek, Paul, Benoît Gaurier, Grégory Germain, Grégory Pinon and Elie Rivoalena (2014). 'Experimental study of the turbulence intensity effects on marine current turbines behaviour. Part I: One single turbine'. In: *Renewable Energy* 66, pp. 729–746 (p. 18).

Nakagawa, H. and Iehisa Nezu (1977). 'Prediction of the contributions to the Reynolds stress from bursting events in open-channel flows'. In: *Journal of Fluid Mechanics* 80.1, pp. 99–128 (p. 10).

Nimmo Smith, W. A. M. (2000). 'Dispersion of material by wind and tide in shallow seas'. PhD thesis, p. 149 (p. 14).

Nimmo Smith, W. A. M., S. A. Thorpe and A. Graham (1999). 'Surface effects of bottom-generated turbulence in a shallow tidal sea'. In: *Nature* 400.6741, pp. 251–254 (p. 14, 15, 24, 25).

Omidyeganeh, M. and U. Piomelli (2011). 'Large Eddies in the Flow over Two-Dimensional Dunes'. In: *Bulletin of the American Physical Society* 56, pp. 1–6 (p. 16).

Ouro, Pablo and Thorsten Stoesser (2019). 'Impact of Environmental Turbulence on the Performance and Loadings of a Tidal Stream Turbine'. In: *Flow, Turbulence and Combustion* 102.3, pp. 613–639 (p. 18, 24, 27).

Phillips, O. M. (1967). 'The maintenance of Reynolds stress in turbulent shear flow'. In: *J. Fluid Mech.* 27.1, pp. 131–144 (p. 7).

Pierrehumbert, R. T. and S. E. Widnall (1982). 'The two and three dimensional instabilities of a spatially periodic shear layer'. In: *Journal of Fluid Mechanics* 114.1, pp. 59–82 (p. 12).

Pieterse, A, JF Filipot, C Maisondieu, L Kilcher and N Chaplain (2017). 'Coupled ADCP measurements for tidal turbulence characterization'. In: *European Wave and Tidal Energy Conference Proceeding*, pp. 28–31 (p. 18).

Prandtl, L. (1904). 'Verhandlungen des dritten internationalen Mathematiker-Kongresses in Heidelberg'. In: *Proc. 3rd Int. Math. Congr.* Heidelberg, Germany, p. 484 (p. 6).

Raupach, M. R., R. A. Antonia and S. Rajagopalan (1991). 'Rough-Wall Turbulent Boundary Layers'. In: *Applied Mechanics Reviews* 44.1, p. 1 (p. 7, 9–12).

Richardson, Lewis F. (1922). *Weather prediction by numerical process*. Cambridge University Press, p. 236 (p. 32).

Rippeth, T. P., J. H. Simpson, E Williams and Mark E. Inall (2003). 'Measurement of the rates of production and dissipation of turbulent kinetic energy in an energetic tidal flow: Red Wharf Bay revisited'. English. In: *Journal of Physical Oceanography* 33.9, pp. 1889–1901 (p. 5, 6).

Rippeth, T. P., E Williams and J. H. Simpson (2002). 'Reynolds stress and turbulent energy production in a tidal channel'. English. In: *Journal of Physical Oceanography* 32.4, pp. 1242–1251 (p. 5).

Robinson, S. K. (1990). 'A Review of Vortex Structures and Associated Coherent Motions in Turbulent Boundary Layers'. In: *Structure of Turbulence and Drag Reduction*, pp. 23–50 (p. 11).

Salim, S., C. Pattiaratchi, R. Tinoco, G. Coco, Y. Hetzel, S. Wijeratne and R. Jayaratne (2017). 'The influence of turbulent bursting on sediment resuspension under unidirectional currents'. In: *Earth Surface Dynamics* 5.3, pp. 399–415 (p. 17, 24, 26).

Scannell, Brian D., T. P. Rippeth, John H. Simpson, Jeff A. Polton and Joanne E. Hopkins (2017). 'Correcting surface wave bias in structure function estimates of turbulent kinetic energy dissipation rate'. In: *Journal of Atmospheric and Oceanic Technology* 34.10, pp. 2257–2273 (p. 6).

Schmidt, M. (2015). *Theoretical Oceanography*, p. 132 (p. 31).

Schubert, G. and G. M Corcus (1967). 'No Title'. In: *J. Fluid Mech.* 29.113 (p. 7).

Secretariat, UNFCCC (1994). *United Nations Framework Convention on Climate Change* (p. 1).

– (1998). *Kyoto Protocol to the United Nations Framework Convention on Climate Change* (p. 1).

Sentchev, A. V., Maxime Thiébaut and François G. Schmitt (2020). 'Impact of turbulence on power production by a free-stream tidal turbine in real sea conditions'. In: *Renewable Energy* 147, pp. 1932–1940 (p. 18).

Soulsby, R. L. (1977). *Similarity Scaling of Turbulence Spectra in Marine and Atmospheric Boundary Layers* (p. 13).

Stacey, Mark T., G Monismith and Jon R Burau (1999). 'Measurements of Reynolds stress profiles in unstratified tidal flow'. In: *Journal of Geophysical Research-Oceans* 104, pp. 933–949 (p. 5).

Sternberg, J. (1967). 'On the interpretation of space-time correlation measurements in shear flow'. In: *Physics of Fluids* 10.9 (p. 7).

Stewart, R. W. (1969). *film notes for: Turbulence* (p. 31).

Sukhodolov, Alexander N., Vladimir I. Nikora and Viktor M. Katolikov (2011). 'Flow dynamics in alluvial channels: The legacy of Kirill V. Grishanin'. In: *Journal of Hydraulic Research* 49.3, pp. 285–292 (p. 25).

Talke, S. A., A. R. Horner-Devine, C. C. Chickadel and A. T. Jessup (2013). 'Turbulent kinetic energy and coherent structures in a tidal river'. In: *Journal of Geophysical Research: Oceans* 118.12, pp. 6965–6981 (p. 15, 16).

Taylor, G. I. (1935). 'Statistical Theory of Turbulence - II'. In: *Proc. R. Soc. Lond. A* 151.873, pp. 421–444 (p. 33).

Tennekes, H. and J. L. Lumley (1972). *A First Course in Turbulence*, p. 300 (p. 29, 32).

Thiébaut, Maxime, Jean François Filipot, Christophe Maisondieu, Guillaume Damblans, Rui Duarte, Eloi Droniou, Nicolas Chaplain, Sylvain Guillou, Jean-François Filipota, Christophe Maisondieub, Guillaume Damblansa, Rui Duartea, Eloi Droniouc and Nicolas Chaplaind (2019). 'A comprehensive assessment of turbulence at a tidal-stream energy site influenced by wind-generated ocean waves'. In: *Energy* 191.November (p. 18).

Thomson, Jim, B. Polagye, Vibhav Durgesh and Marshall C. Richmond (2012). 'Measurements of turbulence at two tidal energy sites in puget sound, WA'. In: *IEEE Journal of Oceanic Engineering* 37.3, pp. 363–374 (p. 17, 18, 26).

Thomson, Jim, B. Polagye, Marshall Richmond and Vibhav Durgesh (2010). 'Quantifying turbulence for tidal power applications'. In: *MTS/IEEE Seattle, OCEANS 2010* 4 (p. 17, 18, 26).

Thorpe, S. A., M. Green, J. H. Simpson, T. R. Osborn and W. A. M. Nimmo Smith (2008). 'Boils and turbulence in a weakly stratified shallow tidal sea.' In: *Journal of Physical Oceanography* 38, pp. 1711–1730 (p. 14, 16, 25).

Townsend, A. A. (1956). 'The properties of equilibrium boundary layers'. In: *Journal of Fluid Mechanics* 1.6, pp. 561–573 (p. 7).

– (1958). 'The turbulent boundary layer'. In: *Boundary Layer Research*. Ed. by Springer, pp. 1–15 (p. 7).

– (1961). 'Equilibrium layers and wall turbulence'. In: *Journal of Fluid Mechanics* 11.1, pp. 97–120 (p. 7).

– (1976). *The structure of turbulent shear flow*, p. 429 (p. 13, 33).

Tritton, J. (1966). 'Some new correlation measurements in a turbulent boundary layer'. In: *J. Fluid Mech.* 28.3, pp. 439–462 (p. 8).

Uihlein, Andreas and Davide Magagna (2016). ‘Wave and tidal current energy - A review of the current state of research beyond technology’. In: *Renewable and Sustainable Energy Reviews* 58, pp. 1070–1081 (p. 3).

Walker-Springett, G. (2020). *Bathymetry dataset* (p. 27).

Walter, R. K., N. J. Nidzieko and S. G. Monismith (2011). ‘Similarity scaling of turbulence spectra and cospectra in a shallow tidal flow’. In: *Journal of Geophysical Research: Oceans* 116.10, pp. 1–14 (p. 9, 13).

Webb, E. K. (1964). ‘Ratio of Spectrum and Structure-Function Constants in the Inertial Subrange’. In: *Q J R Meteorol Soc* 90.385, pp. 344–346 (p. 17).

Wiles, P. J., T. P. Rippeth, John. H. Simpson and P J Hendricks (2006). ‘A novel technique for measuring the rate of turbulent dissipation in the marine environment’. English. In: *Geophysical Research Letters* 33.21 (p. 5).

Willmarth, W. N. and B. J. Tu (1967). ‘Structure of Turbulence in the Boundary Layer near the Wall’. In: *Phys. Fluids* 10.S 134 (p. 7).

Willmarth, W. N. and C. E. Wooldridge (1962). ‘Structure of the Reynolds stress near the wall’. In: *J. Fluid Mech.* 55.1, pp. 65–92 (p. 7).

Wills, J. A. B. (1967). *Spurious Pressure Fluctuations in Wind Tunnels*. Tech. rep. Nat. Phys. Lab. Aero. Rep, p. 13 (p. 7).

Wygnanski, I. and H. Fiedler (1970). ‘The two-dimensional mixing region’. In: *J. Pluid Mech* 41.2, pp. 327–361 (p. 12).